

Prediction of groundwater drawdown using artificial neural networks

Vahid Gholami (✉ Gholami.vahid@guilan.ac.ir)

University of Guilan

Hossein Sahour

The University of Texas at Austin Marine Science Institute

Research Article

Keywords: Groundwater depth, Exploitation, Annual drawdown map, GIS

Posted Date: April 23rd, 2021

DOI: <https://doi.org/10.21203/rs.3.rs-365925/v1>

License:  This work is licensed under a Creative Commons Attribution 4.0 International License. [Read Full License](#)

Version of Record: A version of this preprint was published at Environmental Science and Pollution Research on January 14th, 2022. See the published version at <https://doi.org/10.1007/s11356-021-18115-9>.

Abstract

Groundwater drawdown is typically measured using pumping tests and field experiments; however, the traditional methods are time-consuming and costly when applied to extensive areas. In this research, a methodology is introduced based on artificial neural network (ANN)s and field measurements in an alluvial aquifer in the north of Iran. First, the annual drawdown as the output of the ANN models in 250 piezometric wells was measured, and the data were divided into three categories of training data, cross-validation data, and test data. Then, the effective factors in groundwater drawdown including groundwater depth, annual precipitation, annual evaporation, the transmissivity of the aquifer formation, elevation, distance from the sea, distance from water sources (recharge), population density, and groundwater extraction in the influence radius of each well (1000 m) were identified and used as the inputs of the ANN models. Several ANN methods were evaluated, and the predictions were compared with the observations. Results show that, the modular neural network (MNN) showed the highest performance in modeling groundwater drawdown (Training R-sqr = 0.96, test R-sqr = 0.81). The optimum network was fitted to available input data to map the annual drawdown across the entire aquifer. The accuracy assessment of the final map yielded favorable results (R-sqr = 0.8). The adopted methodology can be applied for the prediction of groundwater drawdown in the study site and similar settings elsewhere.

1. Introduction

Groundwater is the major water resource in arid and semi-arid areas of the world since these resources are less affected by evaporation and pollutants (Wada et al. 2010). Unfortunately, the increase in human population and agricultural and industrial developments have led to an increase in groundwater withdrawal, pollution, and depletion of these resources (Shivasorupy et al. 2012). Moreover, climate change and alteration of precipitation patterns have exerted extra pressure on groundwater resources in these regions making aquifers depletions a serious threat to human life (Abulibdeh et al. 2021). Therefore, access to groundwater fluctuations data and aquifer drawdown is essential for water resources management plans. Unfortunately, these data are often constrained by spatial and temporal gaps in many parts of the world. Even in areas with available groundwater observation networks, the estimation of groundwater drawdown is challenging when applied to a large domain. The use of artificial intelligence (AI) based models in groundwater studies has been growing in the past decade. Different methods of AI, including artificial neural networks (ANNs), fuzzy-neural networks, self-organized maps (SOM), and machine learning (ML), have been applied extensively in the groundwater modeling process. AI-based models have been used in groundwater quality studies (Chou 2006; Chou 2007; Han et al. 2011; Wang et al. 2014; Li et al. 2020; Maliqi et al. 2020; Pal and Chakrabarty 2020; Mosaffa et al. 2021), groundwater depth studies (Dixon 2004; Awasthi et al. 2005; Saemi and Ahmadi 2008; Shiri et al. 2013; Gong et al. 2018; Chen et al. 2020), and the other hydrological studies (Smith and Eli 1995; Dawson 1998; Cheng et al. 2002; Chau and Cheng 2002; Mehr et al. 2003; Wilby et al. 2003; Jain et al. 2004; Ancil and Rat 2005; Cheng et al. 2005; Peters et al. 2006; Demirel et al. 2009; Nourani et al. 2011; Can et al. 2012; Demirel et al. 2012; Kisi et al. 2013; Nourani et al. 2013; Kisi 2015; Taormina and Chau 2015; Nourani et al. 2017 & 2018; Nourani et al. 2019 a&b).

Ghose et al. (2010) used ANN for simulating water table in the region of Orissa and they found that the ANN is very efficient in water table simulation. Wang et al. (2013) used a numerical model for evaluating the dewatering-induced groundwater drawdown. They simulated the relationship between groundwater drawdown and stratum deformation. They indicated that groundwater extraction caused a notable drawdown in the pumping location. Pradhan et al. (2018) evaluated the groundwater extraction status and predicted groundwater level fluctuations using different AI methods such as radial basis function network (RBFN), neuro-fuzzy inference system, and fuzzy logic in an Indian inter-basin. Their results showed the higher performance of the fuzzy logic based model over the neuro-fuzzy and RBFN models in water table modeling. Combining AI-based models with GIS capabilities is a common exercise in groundwater modeling. Previous studies have shown the high performance of this exercise in modeling the quantity and quality of groundwater resources (Tweed et al. 2007; Ganapuram et al. 2009; Arslan 2012; Bradai et al. 2016; Haselbeck et al. 2019; Sahour et al. 2020; Abulibdeh et al. 2021).

The aquifer type and conditions, including the hydrodynamic characteristics of an aquifer, determine the natural recharge potential and fluctuations of the groundwater level (Rukundo and Dogan 2019; Abd-Elhamid et al. 2020; Hereher and Al-Awadhi 2020).

Distance from water resources (such as lakes and rivers), the location of groundwater withdrawal sites, and precipitation values affect the amount of groundwater recharge (Guevara-Ochoa et al. 2018; Shi et al. 2021). Numerous studies have been performed to simulate the fluctuations of groundwater depth; however, estimation of annual drawdown values is challenging because of the complexity of the controlling factors and the needs for various inputs in the modeling process. This study aims to evaluate several ANN methods to predict the spatial variation of the annual groundwater drawdown using its affecting factors in an alluvial aquifer (unconfined aquifer) on the southern coasts of the Caspian Sea.

2. Materials And Method

2.1. Study area

The study area includes a plain with an area of 10000 square kilometers in the north of Iran.

This plain is located on the southern coasts of the Caspian Sea, extending from 50°34' E to 54°10' E and 35°47' N to 37° N (Fig. 1).

The mean annual precipitation of the study area varies from 1300 mm in the west to 600 mm in the east. Rainfall is a common type of precipitation in the Mazandaran plain, and snowfall is rare.

The major types of land uses of the plain are agricultural lands (rice fields and gardens), residential areas (cities and villages) and water bodies (rivers and wetlands), forests, and industrial lands. Geologically, the plain is composed of Quaternary alluvial sediments, and there is an unconfined aquifer in an alluvial aquifer with shallow groundwater. Groundwater depth varies between 1 to 30 meters. The agricultural section is the main consumer of water in the study area, and the main consumption is related to rice fields. The need for groundwater in the agricultural, residential, and industrial sectors in the region is very high.

Due to the existence of more than 300,000 hectares of agricultural lands, the uncontrolled development of tourism and construction, and population growth, this region has faced an increase in water demand and groundwater exploitation. This has led the groundwater resources to experience a significant drawdown and decline in water table across the region (Gholami et al. 2015).

2.2. Measurement of annual groundwater drawdown

To measure the values of groundwater drawdown, 250 piezometric wells in the plain were selected. The location of piezometric wells is shown in Figure (1). The secondary data of monthly groundwater levels in those wells in a period of 5 years (2015 to 2020) were obtained from Mazandaran Regional Water Company (MRWC 2020) and the Water Resources Research Organization of Iran (TAMAB 2020). The difference between groundwater level at its maximum (early spring) and minimum (early autumn) was determined as the values of the annual drawdown. At the beginning of spring, the water table is at its highest due to precipitation and pausing on agricultural activities during the cold seasons. The groundwater in the region is recharged during the six rainy months (Shiri et al. 2013). During the warm seasons (late summer and early fall), low precipitation rates and high agricultural activities, and extraction of groundwater leads to a decline in the water table (Yan et al. 2015). The study period was normal in terms of precipitation and climate without any drought period.

The drawdown values of the examined wells have changed during the 5 years due to changes in precipitation values and agricultural lands as well as the development of residential areas.

Therefore, the mean annual drawdown in this five-year period was determined as the groundwater drawdown values at the location of each well, and the effective factors in groundwater drawdown were quantitatively estimated.

2.3. Factors affecting groundwater drawdown

In this study, the factors affecting groundwater drawdown including extraction values, the transmissivity of aquifer formation, depth to the water table, topography (slope and elevation), location in the watershed, distance from water resources (groundwater recharge), annual precipitation, annual evaporation, and distance from industries and residential centers were used as the inputs of the modeling process (Awasthi et al. 2005; Shiri et al. 2013; Gong et al. 2018; Guevara-Ochoa et al. 2018; Pradhan et al. 2018; Abd-Elhamid et al. 2020; Shi et al. 2021). Examples of inputs are shown in Table (1).

2.3.1. Groundwater level

Groundwater level is one of the main factors affecting the groundwater extraction values (Adamowski and Chan 2011).

Based on the secondary data of the observed groundwater level (water table) in the examined wells, the mean groundwater levels were determined.

Then, using the interpolation of the mean values at each point and the interpolation capabilities of the GIS, the spatial distribution of annual groundwater depth in the Mazandaran plain was estimated.

2.3.2. Transmissivity of aquifer formations

Transmissivity of aquifer formations affects the permeability and the influence radius of the wells (Shie et al. 2016; Gholami et al. 2020).

The aquifer transmissivity in each well was determined using pumping tests conducted by MRWC.

Then, the mean transmissivity map of the entire aquifer was provided using the values of each well and determination of homogeneous areas of transmissivity using geological and hydrogeological maps. The homogeneous areas of transmissivity were prepared and confirmed by MRWC.

2.3.3. Groundwater withdrawal

Determining groundwater extraction is one of the most challenging inputs.

Access to accurate data on exploitation, especially in the case of agricultural wells in the region, was difficult due to the lack of automatic gauges.

For this purpose, data of all rural and urban drinking water wells as well as industrial wells were provided, and their annual extraction values were determined. Further, an accurate digital cadastral map was prepared in the study plain (accuracy 1 meter), which identified all land uses, especially rice fields and gardens.

The maximum influence radius of the wells is considered to be 1000 meters (Shi et al. 2016). Finally, the summation of the groundwater withdrawal was considered as the annual extraction values.

It is noteworthy that according to studies, the water need for one hectare of rice field and one hectare of the garden is about 11,000 and 5,000 m³/year, respectively (MRWC).

As noted above, measuring groundwater withdrawal is very difficult and requires extensive data. In this study, extensive groundwater extraction data from drinking, agricultural, and industrial water wells within the influence radius of the wells were provided.

To prepare a map of groundwater withdrawal within the influence radius of the well, digital layers of agricultural land (rice lands and gardens) and the location and rates of wells were provided in GIS. Since the maximum influence radius of the wells is 1000 meters, therefore, for a 2000 m pixel (sides 1000 meters), the area of agricultural lands was multiplied by their water consumption.

Then, the map of annual groundwater withdrawal within the influence radius was provided as the total consumption rate of agricultural lands.

2.3.4. Annual precipitation and evaporation

Precipitation and evaporation are two affecting factors in groundwater recharge (Guevara-Ochoa et al. 2018).

To estimate the spatial distribution of precipitation and evaporation in the study area, the field-based precipitation and evaporation data were interpolated in the GIS environment to provide the raster layers of annual mean precipitation and evaporation rates.

2.3.5. Topography

Slope affects the hydrogeological conditions in a coastal aquifer (Abd-Elhamid et al. 2020). A 10 m digital elevation model (DEM) was generated using 10 meter contour lines within the GIS. Then, a slope map was provided using DEM and GIS. Further, the spatial location of the wells in the watershed was defined based on the distance from the Caspian Sea or the watershed outlet.

2.3.6. Distance from water sources

All rivers, wetlands, and lakes of the study site were surveyed based on topographic maps and satellite images, and a distance from the water resources map was prepared in the GIS environment. The distance from water resources can be effective in groundwater recharge and depletion (Awasthi et al. 2005).

2.3.7. Distance from industries and residential centers

A database of the plain's industries has been prepared and checked on satellite images.

Residential areas were prepared based on remote sensing and topographic maps with a scale of 25,000. Then, distance from industries and residential areas were prepared in the GIS environment. The wells near industrial and residential areas have a high pumping discharge and can affect the groundwater level (Gholami et al. 2015).

2.4. Prediction of groundwater drawdown by using ANN

The first step is to normalize the data and were randomly divided into three classes: training class (65 percent of the data), cross-validation class (10 percent of the data), and test class (25 percent of the data). Correlation analysis between groundwater drawdown and its affecting factors was conducted to evaluate the network inputs and determine the main factors of groundwater drawdown. NeuroSolutions software was used for the modeling process with different ANNs. In the neural network environment, different structures of inputs were used using the trial-error method and evaluation of network performance. Moreover, the trial-error method was used to determine the optimal architecture of the selected networks, including optimal transfer function, learning technique, neurons number, and number of training epochs. Sensitivity analysis was performed to evaluate the optimal inputs. The goal was to achieve a network that has the highest performance and minimum error in the modeling process. Evaluation criteria of the network performance were the correlation between the predicted and the measured values as well as the error indices such as the coefficient of determination (R-sqr) and the mean squared error (MSE).

Different structure of ANNs including multilayer perceptron (MLP), Jordan and Elman Network (JEN), generalized feed-forward (GFF), radial basis function (RFB), time-lagged recurrent (TLRN), principal component analysis (PCA), and modular neural network (MNN) were used for modeling groundwater drawdown. The multilayer perceptron network typically relies on the back propagation algorithm. The main problems of MLP network are low training speed and need to a large number of training data (Gholami et al. 2020). The JE network develops the MLP with processing elements (PEs). PEs create a network with the ability to extract temporal data from the input data (Mohamed and Atta 2010). The GFF network has a similar structure to the MLP network how connections can go through one or more layers. In fact, the ability of the MLP network to solve problems is not the secret of the GFF network. But, GFF is often much more efficient in solving problems (Beghdad 2008). An MNN is an ANN specialized through a series of independent ANNs moderated by a number of intermediaries.

The intermediaries take the module output and processes them to create an output of the ANN as a whole. Further, the intermediaries only receive the outputs of the modules and does not respond to the modules that do not interact with each other (Bart and Jacob 1994).

The RBF includes a nonlinear hybrid network that is typically comprised of a single hidden layer of the PEs. One of the advantages of this network is its faster processing compared to the MLP network. The TLRN network includes an algorithm with short memory. The TLRN network is developed in nonlinear time series predicting, temporal pattern classification, and identification systems (Sattari et al. 2011). Supervised and unsupervised learning techniques are integrated in the same topology in a PCA network. In fact, the PCA finds a series of uncorrelated features among the inputs and that is an unsupervised linear procedure (Beghdad 2008).

2.5. Performance evaluation of the models

Statistical indices such as the coefficient of determination (R-sqr), the mean absolute error (MAE), the mean squared error (MSE), the Nash–Sutcliffe efficiency (NSE), and matching and correlation between the measured and predicted rates in modeling stages have been used to evaluate the performance of the used networks. Moreover, the observed and predicted values of groundwater drawdown layers were displayed in GIS for comparison and visual evaluation.

3. Results

The mean annual drawdown rates of groundwater in the study region according to the statistics of groundwater depth fluctuations in 250 piezometric wells was between 0.15 to 4.37 meters per year.

The average drawdown in these wells was 1.75 meters per year. A drawdown of about seven meters in a particular year has been observed in some wells. The elevation of the Mazandaran plain varies between - 27 to 30 meters with an average slope of less than 5 percent.

The model inputs such as distance from water resources, distance from industrial centers and population centers vary from zero to several kilometers. Further, the mean annual depth to the water table in the studied plain varies from 0.5 to 40 meters (Fig. 2). The shallow groundwater is observed on the coasts of the Caspian Sea or the outlet of watersheds, and the deepest groundwater is observed in the southern border of Mazandaran plain. The mean annual precipitation and evaporation vary between 600 to 1300 mm and 875 to 1000 mm, respectively.

The annual groundwater extraction within the influence radius of the sampling wells was estimated between 0.1 to 3.66 million m³/year (average 2 million m³/year). The maximum extraction values occur around rice lands and drinking water supply wells (Fig. 2). An example of the estimated data on the inputs and output of neural networks is presented in Table (1). Correlation analysis between inputs and network output was used to find the optimal inputs and the main factors of groundwater drawdown in the region (Table 2).

According to Table 2, factors such as groundwater extraction values, depth to groundwater, and transmissivity of aquifer formations have the highest correlation coefficients.

Therefore, these three factors will be the most important factors in the drawdown of groundwater depth (Pradhan et al. 2018; Abd-Elhamid et al. 2020; Shi et al. 2021)

The results also indicated that the hyperbolic tangent transfer function or sigmoid function and LM learning technique are the best selections for the optimal network structure, which in previous studies were also among the optimum options (Gholami et al. 2021). Different results were obtained during the trial-error procedure with different neural network structures, transfer functions, learning techniques, and the number of neurons. Neural network training in two stages of cross-validation and training yielded favorable results (Table 3). According to the results, all tested neural networks showed acceptable performance in simulating groundwater drawdown. However, the MNN and MLP networks have the highest correlation between the measured and predicted values and the lowest error in the predicted values. Results of the evaluation on the test stage are presented in Table (4).

According to the statistical criteria in Table 4, the MNN network is the most efficient network among the tested networks in predicting the water table drawdown.

The comparison between the predicted and the observed values of groundwater drawdown in the test stage in different structures of the neural network is presented in Figure (3). As can be seen, the MNN network has the highest correlation between the predicted and the observed values. As we mentioned before, the raster layers of optimal network inputs (depth to groundwater, transmissivity, and annual extraction values) were prepared in the GIS environment. The values were converted to numerical format to predict the groundwater drawdown values across the entire studied plain. Finally, the predicted values were converted back to raster format in GIS. The predicted values were presented as a map of the annual groundwater drawdown values (Fig. 4).

The comparison of the predicted and observed groundwater drawdown values (Fig. 4) indicates the accuracy of the results and the performance of the used methodology.

Based on the results, the MNN network has the highest performance and the lowest error in the modeling process (training and testing stages).

4. Discussion

The measured values of groundwater in the wells showed a decline of more than 1.7 m in most parts of the area of the study.

The maximum groundwater drawdown values occur in places with high groundwater depth, high transmissivity (coarse texture), and high groundwater extraction.

According to Table (1), depth to groundwater, extraction values, the transmissivity of aquifer formations, annual precipitation, and evaporation, location elevation, distance from industries and residential centers have a significant relationship with drawdown. The three factors of transmissivity of aquifer formations, exploitation values, and groundwater depth with correlation coefficients of 0.8, 0.7, and 0.6, respectively, were the most effective controlling factors in groundwater drawdown in the study area. The higher the transmissivity or permeability of the aquifer, the higher the possibility of extraction with higher pumping discharge, and as a result, we will see a higher decline in the water table (Pradhan et al. 2018). In fact, high transmissivity leads to a larger influence radius in a well. Therefore, groundwater extraction, even at a further distance, affects the water table in adjacent areas. According to the results, the amount of groundwater withdrawal is also directly related to the decline of the groundwater table (Awasthi et al. 2005; Saemi et al. 2008; Gong et al. 2018).

Precipitation is one of the main factors of the natural recharge of groundwater. A significant and inverse relationship between precipitation and groundwater drawdown values was reported in previous studies (Shiri et al. 2013). However, this relationship was not meaningful in the study area since there is no significant variation in precipitation to be correlated with the change in water table.

Evaporation can affect near surface groundwater or in the areas where groundwater meet surface water such as wetlands. However, evaporation is not correlated with groundwater drawdown in the studied plain. The elevation is an effective factor in the water table in unconfined aquifers. Low lands have more water recharge capacity, and the water table is higher in them causing lower decline in water table. The precipitation in these area are high and the gentle topography cause water to have enough time to recharge the groundwater. Also, the areas closer to the Caspian Sea coasts are affected by surface water discharges.

Distance from industries and residential centers are two factors that have a significant relationship.

Because these areas are the place of drilling wells and they reflect the density of withdrawal sites and the extraction values of groundwater (Gholami et al. 2015). The presence of surface water can reduce the reliance and pressure on groundwater resources. Therefore, distance from water resources (rivers, wetlands, freshwater lakes) can play an important role in water table fluctuations.

However, no significant relationship between this parameter and groundwater drawdown values were observed in the studied plain.

The process of predicting groundwater drawdown was performed using different neural networks in which most of them showed an acceptable performance. Previous studies have also indicated the performance of the ANNs in modeling the groundwater depth (Coulialy et al. 2001; Daliakopoulos et al. 2005; Lallahem et al. 2005; Nayak et al. 2006; Krishna et al. 2008; Yoon et al. 20011; Li et al. 2012; Mohanty et al. 2013; Alshehri et al. 2020). Among the various neural network structures used, the MNN network showed the highest efficiency, and the TLRN network had the lowest performance in predicting groundwater drawdown. According to Table (3), there was not much difference between the performance of the tested networks. Correct prediction of the maximum drawdown values is important in water resources management planning. The adopted methodology showed high accuracy in predicting maximum drawdown values.

The study also showed that using only three main inputs (transmissivity, depth to the water table, and extraction rate) and an efficient neural network structure, groundwater drawdown can be predicted with acceptable accuracy. Providing a reliable groundwater drawdown map can help water resource managers adopting strategies to mitigate the impacts of groundwater depletion.

Further, the inputs of groundwater depth and groundwater exploitation values will change over time. The adopted methodology can be used for investigating different scenarios of groundwater withdrawal and climate variability.

5. Conclusion

Assessment of groundwater drawdown is complex and challenging task due to the presence of various climatic and anthropogenic factors. Traditional field-based measurement of groundwater drawdown requires a dense network of observational wells, which is not available in many countries. We adopted a feasible conventional methodology to map a large scale prediction of groundwater drawdown in an alluvial and coastal aquifer. The relationship between groundwater withdrawal and its affecting factors in 250 wells was established using ANN-based models. Using available input data in the study area, the spatial changes of the annual groundwater drawdown was mapped across the entire study area.

In the modeling process, different neural network structures with different inputs can be used. However, the most challenging step is to quantify the parameters that explain the groundwater drawdown in an aquifer in order to train an ANN. The advantages of using artificial intelligence in predicting the groundwater drawdown are speed of operation, high performance, low cost, and connectivity with other systems such as GIS. The adopted methodology can be used to predict changes in groundwater drawdown in the study area and in similar settings elsewhere. This can be performed under different scenarios of climate and groundwater withdrawal. To complete future studies we suggest using other methods of artificial intelligence and machine learning, as well as different input parameters for the prediction of drawdown values.

Declarations

Acknowledgments

We would like to thank the Mazandaran Regional Water Authority and Mazandaran Water and Sewerage Department for providing the hydrogeological and groundwater extraction data.

References

- Abd-Elhamid HF, Abd-Elaty I, Sherif MM (2020) Effects of aquifer bed slope and sea level on saltwater intrusion in coastal aquifers. *J. Hydrol.* 7 (2020), p. 5, 10.3390/hydrology7010005
- Abulibdeh A, Al-Awadhi T, Nasiri N, Buloshi A, Abdelghani M (2021) Spatiotemporal mapping of groundwater salinity in Al-Batinah, Oman. *Groundwater Sustainable Dev.* Vol (12), 2021, 100551. [.org/10.1016/j.gsd.2021.100551](https://doi.org/10.1016/j.gsd.2021.100551).
- Adamowski J, Chan HF (2011) A wavelet neural network conjunction model for groundwater level forecasting. *J Hydrol* 407:28–40
- Alshehri F, Sultan M, Karki S, Alwagdani E, Alsefry S, Alharbi H, Sahour H, Sturchio N (2020) Mapping the distribution of shallow groundwater occurrences using Remote Sensing-based statistical modeling over southwest Saudi Arabia. *Remote Sensing* 12(9), p.1361
- Antcil F, Rat A (2005) Evaluation of neural networks streamflow forecasting on 47 watersheds. *J Hydrol Eng ASCE* 10(1):85–88.DOI: 10.1061/ (ASCE) 1084 – 0699(2005)10:1(85)
- Arsilan H (2012) Spatial and temporal mapping of groundwater salinity using ordinary kriging and indicator kriging: The case of Bafra Plain, Turkey. *Agric Water Manage* 113:57–63
- Awasthi AK, Dubey OP, Awasthi A, Sharma S (2005) A Fuzzy Logic model for estimation of groundwater recharge. In: Annual meeting of the North American fuzzy information processing society, Detroit, MI, June 26–28, 809–813

- Bart H, Jacob M (1994) The design and evolution of modular neural network architectures. *Neural networks* 7(6–7),985–1004. doi:10.1016/s0893-6080(05)80155-8
- Beghdad R (2008) Critical study of neural networks in detecting intrusions. *Computers Security* 27(5):168–175
- Bradaï A, Douaoui A, Bettahar N, Yahiaoui I (2016) Improving the prediction accuracy of groundwater salinity mapping using indicator kriging method. *J Irrig Drain Eng* 142:04016023
- Can I, Tosunoglu F, Kahya E (2012) Daily streamflow modelling using autoregressive moving average and artificial neural networks models: case study of Çoruh basin, Turkey. *Water Environ J* 26(4):567–576
- Cheng CT, Ou CP, Chau KW (2002) Combining a fuzzy optimal model with a genetic algorithm to solve multi-objective rainfall–runoff model calibration. *J hydrol* 268(1–4):72–86
- Cheng CT, Wu XY, Chau KW (2005) Multiple criteria rainfall–runoff model calibration using a parallel genetic algorithm in a cluster of computers Calage multi-critères en modélisation pluie–débit par un algorithme génétique parallèle mis en œuvre par une grappe d'ordinateurs. *Hydrologi Sci J* 50(6):1–1087
- Chen C, He W, Zhou H, Xue Y, Zhu M (2020) A comparative study among machine learning and numerical models for simulating groundwater dynamics in the Heihe River Basin, northwestern China. *Sci Rep* 10:3904. doi:10.1038/s41598-020-60698-9
- Chou K (2006) A review on integration of artificial intelligence into water quality modelling. *Mar poll Bull* 52(7):726–733
- Chou K (2007) An ontology-based knowledge management system for flow and water quality modeling. *Adv Eng Software* 38(3):172–181
- Coulibaly P, Anctil F, Aravena R, Bobee B (2001) Artificial neural network modeling of water table depth fluctuations. *Water Resour Res* 37(4):885–896
- Daliakopoulos IN, Coulibaly P, Tsanis IK (2005) Groundwater level forecasting using artificial neural network. *J Hydrol* 309:229–240
- Dawson CW (1998) An artificial neural network approaches to rainfall runoff modeling. *J Hydrol Sci* 43(1):47–66
- Demirel MC, Venancio A, Kahya E (2009) Flow forecast by SWAT model and ANN in Pracana basin, Portugal. *Adv Eng Software* 40(7):467–473
- Demirel MC, Booij MJ, Kahya E (2012) Validation of an ANN flow prediction model using a multistation cluster analysis. *J hydrol eng* 17(2):262–271
- Dixon B (2004) Prediction of groundwater vulnerability using an integrated GIS-based neuro-fuzzy techniques. *J Spa hydrol* 14(12):1–38
- Ganapuram S, Kumar GT, Krishna IV, Kahya E, Demirel MC (2009) Mapping of groundwater potential zones in the Musi basin using remote sensing data and GIS. *Adv Eng Software* 40(7):506–518
- Gholami V, Agha Goli., Kalteh AM (2015) Modeling sanitary boundaries of drinking water wells on the Caspian Sea southern coasts, Iran. *Environ Earth Sci* 74(4):2981–2990
- Gholami V, Sahour H, Hadian MA (2021) Soil erosion modeling using erosion pins and artificial neural networks. *Catena* (196):104902. doi.org/10.1016/j.catena.2020.104902
- Ghose DK, Panda SS, Swain PC (2010) Prediction of water table depth in western region, Orissa using BPNN and RBF neural networks. *J Hydrol* 394:296–304
- Gong YC, Wang ZJ, Xu GY, Zhang Z (2018) A Comparative study of groundwater level forecasting using data-driven models based on ensemble empirical mode decomposition. *Water* 10:20. doi:10.3390/w10060730
- Guevara-Ochoa C, Medina-Sierra A, Vives L (2018) Spatio-temporal effect of climate change on water balance and interactions between groundwater and surface water in plains. *Sci Total Environ* 722:137886. doi.org /10. 1016/j.scitotenv.2020.137886
- Han HG, Chen QI, Qiao JF (2011) An efficient self-organizing RBF neural network for water quality prediction. *Neural Netw* 24(7):717–725
- Haselbeck V, Kordilla J, Krause F, Sauter M (2019) Self-organizing maps for the identification of groundwater salinity sources based on hydrochemical data. *J Hydrol* 576:610–619
- Hereher M, Al-Awadhi T (2020) Remote sensing of coastal ecosystems using spectral indices ICVISP 2019: Proceedings of the 3rd International Conference on Vision, Image and Signal Processing August 2019 (2020), pp. 1–5, doi:10.1145/3387168.3387174
- Jain A, Sudheer KP, Srinivasulu S (2004) Identification of physical processes inherent in artificial neural network rainfall–runoff models. *Hydrol Process* 118(3):571–581
- Kisi O, Shiri J, Tombul M (2013) Modeling rainfall-runoff process using soft computing techniques. *Comput Geosci* 51:108–117
- Kisi O (2015) Discussion of Improved Particle Swarm Optimization–Based Artificial Neural Network for Rainfall-Runoff Modeling by Mohsen Asadnia, Lloyd HC Chua, XS Qin, and Amin Talei. *J Hydrol Eng* 20(9):07015009

- Krishna B, Satyaji Rao YR, Vijaya T (2008) Modeling groundwater levels in an urban coastal aquifer using artificial neural networks. *Hydrol Process* 22:1180–1188
- Lallahem S, Mania J, Hani A, Najjar Y (2005) On the use of neural networks to evaluate groundwater levels in fractured media. *J Hydrol* 307(1–4):92–111
- Li X, Shu L, Liu L, Yin D, Wen J (2012) Sensitivity analysis of groundwater level in Jinci Spring Basin (China) based on artificial neural network modeling. *Hydrogeol J* 20:727–738
- Li J, Shi Z, Liu F (2020) Evaluating spatiotemporal variations of groundwater quality in northeast Beijing by self-organizing map. *Water* 12(5):1382. doi.org/10.3390/w12051382
- Maliqi E, Jusufi K, Singh SK (2020) Assessment and spatial mapping of groundwater quality parameters using metal pollution indices, graphical methods and geoinformatics. *Anal. Chem. Lett.* 10 (2) (2020), 152–180
- Mazandaran Regional Water Company (MRWC) (2020) Hydrogeologic studies, The monthly data of pizeometric wells, Mazandaran plain
- McGee T (2001) Urbanization takes on new dimensions in Asia's population giants. *Popul Today* 29:1–2. POPLINE Document Number: 161361
- Mehr AD, Kahya E, Olyae E (2003) Stream flow prediction using linear genetic programming in comparison with a neuro-wavelet technique. *J Hydrol* 505:240–249
- Mohamed MA, Atta MM (2010) Automated classification of galaxies using transformed domain features. *IJCSNS International Journal of Computer Science* 86 Network Security (10(2):86–91
- Mohanty S, Madan KJ, Ashwani Kumar, Panda DK (2013) Comparative evaluation of numerical model and artificial neural network for simulating groundwater flow in Kathajodi–Surua Inter-basin of Odisha, India. *J. hydrol.* 495 (2013) 38–51
- Mosaffa M, Nazif S, Amirhosseini YK, Balderer W, Meiman MH (2021) An investigation of the source of salinity in groundwater using stable isotope tracers and GIS: a case study of the Urmia Lake basin, Iran. *Groundwater Sustainable Dev.* 12 (2021), p. 100513
- Nayak PC, Rao YRS, Sudheer KP (2006) Groundwater level forecasting in a shallow aquifer using artificial neural network approach. *Water Resour Manage* 20:77–90
- Nourani V, Kisi O, Komasi (2011) Two hybrid artificial intelligence approaches for modeling rainfall–runoff process. *J Hydrol* 402(1–2):41–59
- Nourani V, Baghanam AH, Vousoughi VD, Alami MT (2012) Classification of groundwater level data using SOM to develop ANN-based forecasting model. *Int J Soft Comput Eng* 2(1):2231–2307
- Nourani V, Baghanam AH, Adamowski J, Gebremichael M (2013) Using self-organizing maps and wavelet transforms for space–time pre-processing of satellite precipitation and runoff data in neural network based rainfall–runoff modeling. *J hydrol* 476:228–243
- Nourani V, Andalib G, Sadikoglu F, Sharghi E (2018) Cascade-based multi-scale AI approach for modeling rainfall-runoff process. *Hydrol Res* 49(4):1191–1207
- Nourani V, Davanlou Tajbakhsh A, Molajou A, Gokcekus H (2019a) Hybrid Wavelet-M5 Model Tree for Rainfall-Runoff Modeling. *J Hydrol Eng* 24(5):04019012
- Nourani V, Tajbakhsh AD, Molajou A (2019b) Data mining based on wavelet and decision tree for rainfall-runoff simulation. *Hydrol Res* 50(1):75–84
- Pal J, Chakrabarty D (2020) Assessment of artificial neural network models based on the simulation of groundwater contaminant transport. *Hydrogeol J* 28(1–2):1–17. doi:10.1007/s10040-020-02180-4
- Peters R, Schmitz G, Cullmann J (2006) Flood routing modelling with Artificial Neural Networks. *Adv Geosci* 9:131–136
- Pradhan S, Kumar S, Kumar Y, Chandra Sharma H (2018) Assessment of groundwater utilization status and prediction of water table depth using different heuristic models in an Indian interbasin. *Soft Computing. Soft Comput.* 23, 10261–10285 (2019). doi.org/10.1007/s00500-018-3580-4
- Rukundo E, Ahmet Dogan A (2019) Dominant influencing factors of groundwater recharge spatial patterns in Ergene River catchment. *Turkey Water* 2019 11:653. doi:10.3390/w11040653
- Saemi M, Ahmadi M (2008) Integration of genetic algorithm and a coactive neuro-fuzzy inference system for permeability prediction from well logs data. *Transp in Porous Media* 71(3):273–288. doi:10.1007/s11242-007-9125-4
- Sahour H, Gholami V, Vazifedan M (2020) A comparative analysis of statistical and machine learning techniques for mapping the spatial distribution of groundwater salinity in a coastal aquifer. *J Hydrol* 591:125321. doi.org/10.1016/j.jhydrol.2020.125321
- Samani N, Gohari-Moghadam M, Safavi AA (2007) A simple neural network model for the determination of aquifer parameters. *J Hydrol* 340:1–11. DOI:10.1007/s10584-005-5922-3

- Sattari MT, Yurekli K, Pal M (2011) Performance evaluation of artificial neural network approaches in forecasting reservoir inflow. *Appl Math Model* 36(6):2649–2657
- Shi X, Jiang S, Xu H, Jiang F, He Z, Wu J (2016) The effects of artificial recharge of groundwater on controlling land subsidence and its influence on groundwater quality and aquifer energy storage in Shanghai, China. *Environ. Earth Sci.* 75, 195 (2016). doi.org/10.1007/s12665-015-5019-x
- Shi W, Lu C, Werner AD (2021) Assessment of the impact of sea-level rise on seawater intrusion in sloping confined coastal aquifers. *J Hydrol* 124872:10 1016 /j. jhydrol.2020.124872
- Shiri J, Kisi O, Yoon H, Lee KK, Hossein Nazemi A (2013) Predicting groundwater level fluctuations with meteorological effect implications—A comparative study among soft computing techniques. *Comput. Geosci.* 56, 32–44, doi.org/10. 1016/j. cageo. 2013.01.007
- Shivasorupy B, Barry J, Mathias Maier L (2012) Sanitary hazards and microbial quality of open dug wells in the Maldives islands. *J. Water Resour. Prot.* (4): 474–486
- Smith J, Eli RN (1995) Neural network models of the rainfall–runoff process. *J Water Resour Plan Manage ASCE* 121:499–508
- TAMAB (Water Resources Research Organization of Iran) (2020) Mazandaran Regional Water Company, Hydrogeology studies of Mazandaran Plain. Atlas report
- Taormina R, Chau KW (2015) Data-driven input variable selection for rainfall–runoff modeling using binary-coded particle swarm optimization and Extreme Learning Machines. *J Hydrol* 529:1617–1632
- Tweed SO, Leblanc M, Webb JA, Lubczynski MW (2007) Remote sensing and GIS for mapping groundwater recharge and discharge areas in salinity prone catchments, southeastern Australia. *Hydrogeol J* 15:75–96
- Wada Y, Van Beek LP, Van Kempen CM, Reckman JW, Vasak S, Bierkens MF (2010) Global depletion of groundwater resources. *J. Water Resour. Prot.* 1, 37. doi. Org/10. 1029/2010GL044571
- Wang W, Xu D, Chau K, Lei G (2014) Assessment of river water quality based on theory of variable fuzzy sets and fuzzy binary comparison method. *Water Resour Manage* 28(12):4183–4200
- Wang D, Li M, Chen J, Xia X, Zhang Y (2019) Numerical study on groundwater drawdown and deformation responses of multilayer strata to pumping in a confined aquifer. *Journal of Shanghai Jiaotong University (Science)* (24):287–293
- Wilby RL, Abrahart RJ, Dawson CW (2003) Detection of conceptual model rainfall–runoff processes inside an artificial neural network. *J Hydrol Sci* 48(2):163–181
- Yan F, Yu S, Wu Y, Pan D, She D, Ji J (2015) Seasonal Variations in Groundwater Level and Salinity in Coastal Plain of Eastern China Influenced by Climate. *J. Chem.* vol. 2015, Article. ID 905190, 8 p, 2015. https://doi.org/10.1155/2015/905190.doi.org /10. 1155/2015/905190
- Yoon H, Jun SC, Hyun Y, Bae GO, Lee KK (2011) A comparative study of artificial neural networks and support vector machines for predicting groundwater levels in a coastal aquifer. *J Hydrol* 396:128–138

Tables

Table (1). A number of the network inputs and output for predicting the groundwater drawdown.

| ID well | Drawdown (m) | Groundwater depth (m) | Transmissivity (m ² /day) | Exploitation (10 ⁶ m ³) | Elevation (m) | Evaporation (mm) | L _{sea} (m) | Precipitation (mm) | Population (people) | L _{settleme} (m) | L _{indus} (m) |
|---------|--------------|-----------------------|--------------------------------------|--|---------------|------------------|----------------------|--------------------|---------------------|---------------------------|------------------------|
| 1 | 2.12 | 18.17 | 1500 | 2.5 | 89 | 953 | 20428 | 806 | 174 | 378 | 343 |
| 2 | 2.87 | 2.57 | 1250 | 2.66 | -5 | 960 | 10279 | 594 | 2568 | 20 | 500 |
| 4 | 1.05 | 3.49 | 300 | 0.3 | -24 | 747 | 854 | 1480 | 5730 | 30 | 40 |
| 5 | 1.60 | 6.67 | 375 | 1.98 | -8 | 995 | 7083 | 620 | 1955 | 12 | 640 |
| 7 | 1.24 | 1.98 | 150 | 1.95 | -5 | 1006 | 18626 | 753 | 323 | 7 | 226 |
| 8 | 0.24 | 0.42 | 75 | 0.3 | 20 | 1024 | 26288 | 833 | 1358 | 30 | 1080 |
| 9 | 3.09 | 37.13 | 2750 | 3.04 | 82 | 998 | 20728 | 818 | 676 | 0 | 780 |
| 15 | 1.79 | 9.02 | 1250 | 1.8 | 40 | 1021 | 33425 | 1036 | 582 | 70 | 377 |
| 16 | 1.33 | 3.75 | 750 | 1.9 | -5 | 961 | 10734 | 822 | 205 | 10 | 590 |
| 17 | 1.26 | 7.80 | 175 | 2.24 | -9 | 1023 | 10288 | 539 | 394 | 22 | 570 |
| 19 | 0.78 | 2.14 | 375 | 2.21 | -21 | 892 | 2214 | 1029 | 1966 | 15 | 693 |
| 20 | 3.00 | 34.70 | 2580 | 3.17 | 108 | 1015 | 26681 | 909 | 1506 | 0 | 405 |
| 21 | 1.58 | 0.77 | 400 | 2.41 | 0 | 1023 | 13945 | 584 | 1215 | 10 | 890 |
| 27 | 1.25 | 1.65 | 500 | 2.89 | 3 | 1029 | 20436 | 643 | 967 | 12 | 1270 |
| 28 | 2.93 | 3.93 | 2000 | 2.85 | 29 | 1024 | 29427 | 889 | 360 | 15 | 600 |
| 31 | 1.09 | 1.75 | 175 | 2.76 | -20 | 1008 | 854 | 985 | 212 | 35 | 1588 |
| 32 | 1.72 | 2.13 | 375 | 2.76 | -8 | 1020 | 10139 | 588 | 837 | 2 | 910 |
| 35 | 0.24 | 0.82 | 75 | 2.6 | -23 | 953 | 1000 | 1163 | 1036 | 3 | 864 |
| 42 | 1.41 | 2.36 | 100 | 2.85 | -25 | 1010 | 922 | 923 | 2950 | 10 | 1393 |
| 49 | 0.77 | 3.43 | 1000 | 1.15 | 31 | 958 | 14277 | 791 | 308 | 50 | 86 |
| 50 | 2.68 | 7.86 | 2000 | 1.55 | 38 | 1021 | 33741 | 1045 | 961 | 0 | 1250 |
| 52 | 0.53 | 1.80 | 750 | 1.13 | -23 | 875 | 1746 | 1006 | 185 | 17 | 979 |
| 53 | 3.25 | 5.03 | 2500 | 3.4 | -7 | 972 | 10412 | 745 | 2850 | 30 | 240 |
| 55 | 1.68 | 1.17 | 500 | 2.43 | -25 | 939 | 5000 | 697 | 1124 | 10 | 1510 |
| 57 | 2.41 | 1.75 | 1500 | 2.32 | 155 | 1001 | 1273 | 503 | 600 | 630 | 610 |
| 58 | 2.37 | 2.36 | 2000 | 1.9 | -15 | 994 | 583 | 462 | 910 | 102 | 188 |
| 60 | 1.72 | 1.93 | 300 | 2.56 | -26 | 944 | 8233 | 656 | 1525 | 660 | 236 |
| 61 | 1.55 | 0.75 | 125 | 2.06 | -26 | 934 | 5728 | 638 | 332 | 4300 | 217 |
| 63 | 2.10 | 21.08 | 2000 | 2.13 | 178 | 1189 | 6768 | 565 | 506 | 1750 | 292 |
| 65 | 2.90 | 11.96 | 2000 | 3.27 | 37 | 1127 | 7710 | 512 | 638 | 2300 | 370 |
| 69 | 4.37 | 36.02 | 3000 | 2.78 | 34 | 993 | 10100 | 737 | 1528 | 10 | 48 |
| 70 | 3.58 | 9.58 | 2500 | 3.38 | 20 | 996 | 8698 | 688 | 1044 | 10 | 366 |
| 77 | 4.08 | 26.28 | 2750 | 2.84 | 24 | 970 | 12816 | 740 | 2930 | 318 | 279 |
| 78 | 2.99 | 3.33 | 2500 | 2.03 | -2 | 982 | 4600 | 556 | 1269 | 378 | 170 |
| 79 | 0.88 | 2.61 | 500 | 1.98 | -19 | 990 | 1118 | 478 | 1100 | 621 | 510 |
| 80 | 2.70 | 2.52 | 1500 | 2.6 | 1 | 1023 | 5412 | 529 | 389 | 1440 | 209 |
| 84 | 3.97 | 26.54 | 3000 | 2.78 | 13 | 973 | 16754 | 747 | 2760 | 15 | 310 |
| 102 | 2.05 | 1.60 | 2000 | 1.64 | -13 | 710 | 1600 | 1298 | 814 | 90 | 480 |
| 103 | 3.40 | 8.00 | 2750 | 1.55 | 36 | 745 | 3900 | 1342 | 1003 | 78 | 336 |
| 122 | 4.08 | 23.20 | 3000 | 2.96 | 30 | 981 | 4880 | 1210 | 450 | 48 | 350 |
| 152 | 1.13 | 1.65 | 175 | 2.27 | -6 | 1001 | 9610 | 611 | 725 | 200 | 474 |
| 169 | 3.36 | 7.76 | 2500 | 2.77 | 12 | 971 | 16274 | 602 | 199 | 27 | 740 |

| | | | | | | | | | | | |
|-----|------|-------|------|------|-----|------|-------|------|------|------|------|
| 218 | 2.72 | 27.19 | 2200 | 3.05 | 144 | 1006 | 24490 | 851 | 1374 | 100 | 5 |
| 222 | 0.20 | 0.48 | 50 | 0.1 | -3 | 862 | 2961 | 903 | 2183 | 3600 | 1560 |
| 232 | 0.34 | 1.12 | 125 | 1.12 | -23 | 849 | 632 | 1004 | 2151 | 9 | 1190 |
| 236 | 0.71 | 2.84 | 100 | 0.62 | -12 | 701 | 500 | 1081 | 490 | 15 | 700 |
| 240 | 0.53 | 1.52 | 750 | 2.4 | 17 | 891 | 11669 | 879 | 386 | 5 | 405 |

Table (2). Correlation matrix of the input variables and the groundwater drawdown.

| Parameter | N=250 | 1 | 2 | 3 | 4 | 5 | 6 | 7 | 8 | 9 | 10 | 11 | 12 | 13 |
|--|-------|-------|--------|-------|-------|-------|--------|-------|-------|--------|--------|------|-------|------|
| 1. Groundwater drawdown | | 1.00 | | | | | | | | | | | | |
| 2. Depth to water table | | 0.60 | 1.00 | | | | | | | | | | | |
| 3. Transmissivity of aquifer formation | | 0.81 | 0.63 | 1.00 | | | | | | | | | | |
| 4. Elevation | | 0.28 | 0.51 | 0.34 | 1.00 | | | | | | | | | |
| 5. Slope | | 0.09 | 0.06 | 0.139 | 0.06 | 1.00 | | | | | | | | |
| 6. Annual evaporation | | 0.26 | 0.18 | 0.12 | 0.23 | -0.03 | 1.00 | | | | | | | |
| 7. Distance from water resources | | -0.01 | -0.11 | -0.02 | -0.17 | 0.01 | -0.006 | 1.00 | | | | | | |
| 8. Distance from sea | | 0.23 | 0.33 | 0.25 | 0.37 | -0.13 | 0.45 | 0.00 | 1.00 | | | | | |
| 9. Annual precipitation | | -0.18 | -0.005 | -0.02 | -0.11 | 0.02 | -0.63 | 0.10 | -0.26 | 1.00 | | | | |
| 10. Population | | 0.20 | 0.16 | 0.15 | -0.06 | -0.03 | 0.02 | 0.10 | 0.06 | -0.052 | 1.00 | | | |
| 11. Distance from residential areas | | 0.05 | 0.01 | 0.01 | 0.08 | 0.04 | 0.12 | 0.00 | -0.15 | -0.171 | -0.006 | 1.00 | | |
| 12. Distance from industries | | -0.27 | -0.19 | -0.20 | -0.14 | -0.05 | -0.12 | -0.05 | -0.17 | 0.08 | -0.18 | 0.00 | 1.00 | |
| 13. Goundwater extraction | | 0.69 | 0.43 | 0.47 | 0.28 | 0.009 | 0.39 | -0.03 | 0.233 | -0.37 | 0.17 | 0.07 | -0.22 | 1.00 |

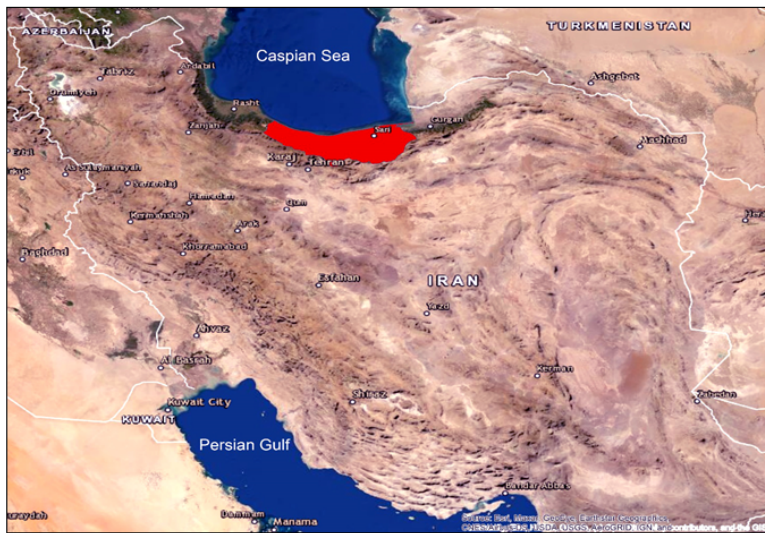
Table (3). Evaluating the performance of the used ANN methods in the training and cross-validation phase for predicting the groundwater drawdown.

| R-sqr | NSE | Final MSE | The minimum MSE | Prediction stage | ANN network |
|-------|------|-----------|-----------------|------------------|-------------|
| | 0.89 | 0.001 | 0.006 | Training | GFF |
| 0.88 | | 0.0001 | 0.005 | Cross-validation | |
| | 0.96 | 0.0001 | 0.004 | Training | MLP |
| 0.95 | | 0.0002 | 0.004 | Cross-validation | |
| | 0.88 | 0.0000 | 0.004 | Training | JEN |
| 0.87 | | 0.0001 | 0.005 | Cross-validation | |
| | 0.9 | 0.0000 | 0.004 | Training | RFB |
| 0.88 | | 0.0000 | 0.005 | Cross-validation | |
| | 0.97 | 0.0001 | 0.001 | Training | MNN |
| 0.96 | | 0.0002 | 0.004 | Cross-validation | |
| | 0.85 | 0.0000 | 0.004 | Training | PCA |
| 0.86 | | 0.0002 | 0.005 | Cross-validation | |
| | 0.76 | 0.001 | 0.02 | Training | TLRN |
| 0.75 | | 0.002 | 0.03 | Cross-validation | |

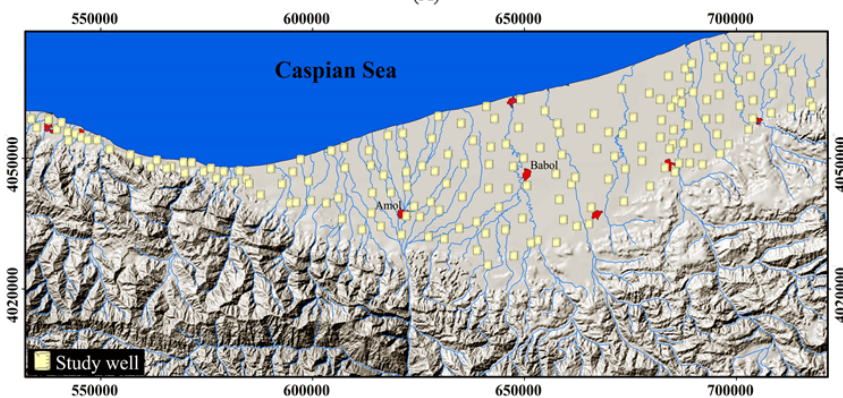
Table (4) Evaluating the performance of the used ANN methods in the testing or validation stage for predicting the groundwater drawdown.

| R-sqr | NSE | ME | MSE | ANN |
|-------|------|------|------|------|
| 0.79 | 0.78 | 0.34 | 0.18 | GFF |
| 0.8 | 0.8 | 0.34 | 0.18 | MLP |
| 0.77 | 0.79 | 0.35 | 0.19 | JEN |
| 0.77 | 0.73 | 0.38 | 0.21 | RFB |
| 0.81 | 0.81 | 0.32 | 0.17 | MNN |
| 0.78 | 0.78 | 0.35 | 0.19 | PCA |
| 0.66 | 0.65 | 0.41 | 0.31 | TLRN |

Figures



(A)



(B)

Figure 1
 Geographical location of the study plain (A), and the studied wells on the southern coasts of Caspian Sea (B). Note: The designations employed and the presentation of the material on this map do not imply the expression of any opinion whatsoever on the part of Research Square concerning the legal status of any country, territory, city or area or of its authorities, or concerning the delimitation of its frontiers or boundaries. This map has been provided by the authors.

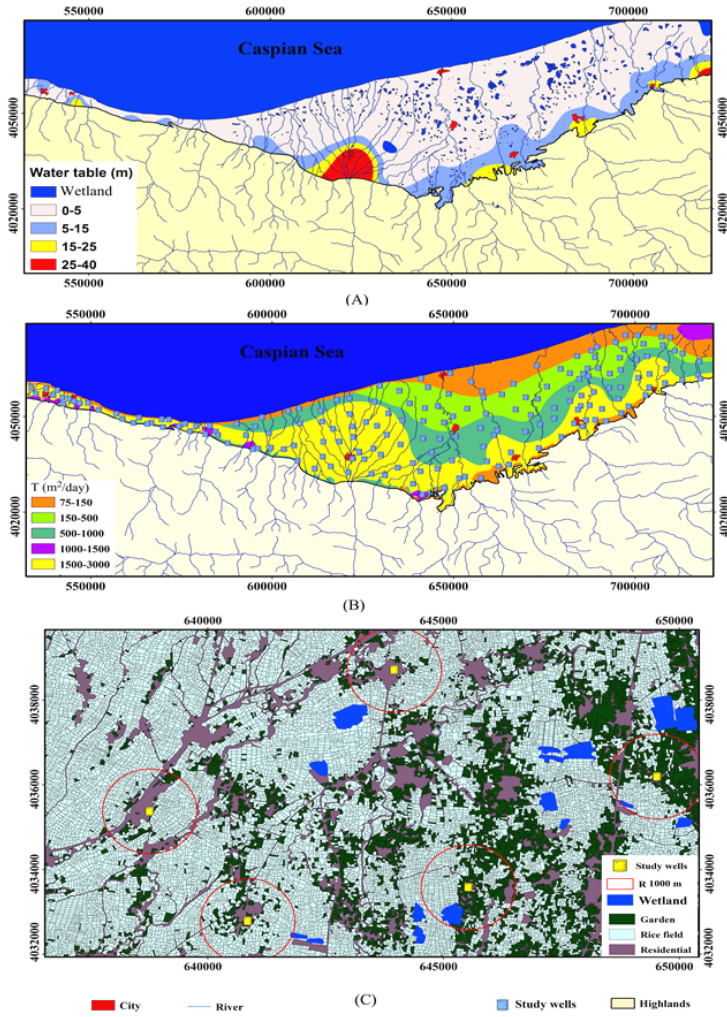


Figure 2

(A) The mean depth to water table (m); (B) The spatial variation of the mean transmissivity of aquifer formation (m²/day); (C) A view of the study area showing the location of sampling wells and different types of land uses (groundwater exploitation estimation). Note: The designations employed and the presentation of the material on this map do not imply the expression of any opinion whatsoever on the part of Research Square concerning the legal status of any country, territory, city or area or of its authorities, or concerning the delimitation of its frontiers or boundaries. This map has been provided by the authors.

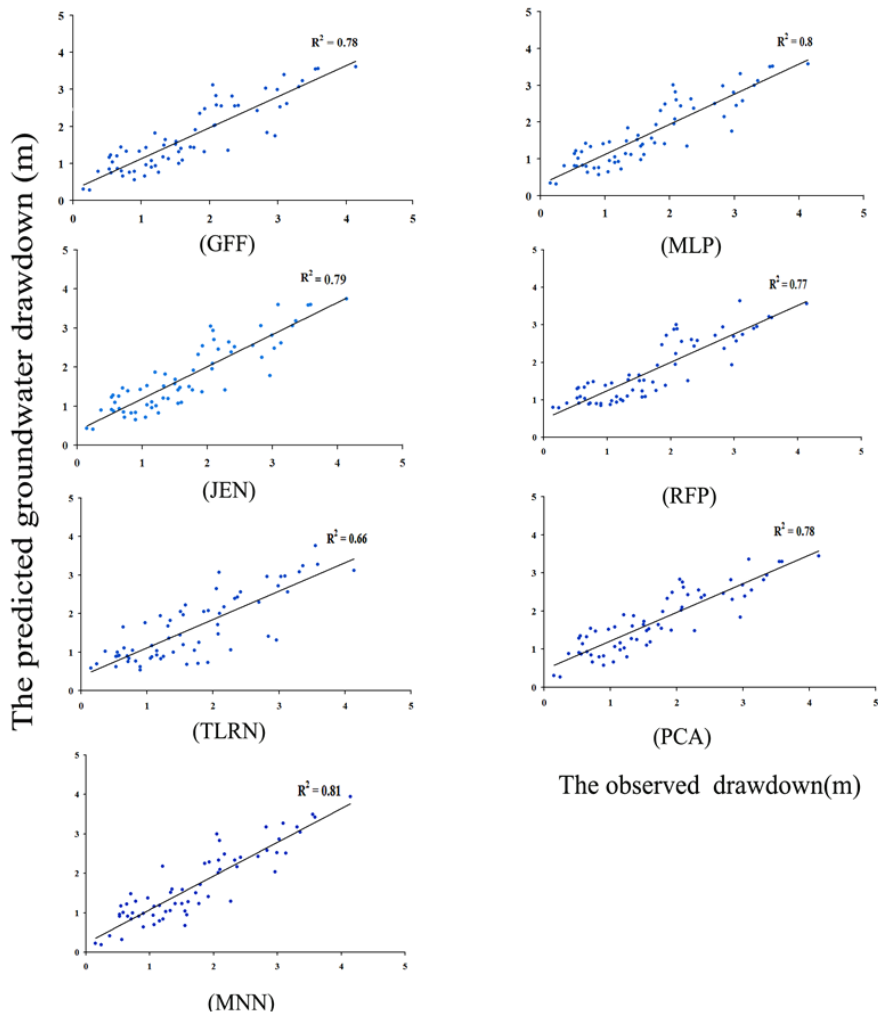


Figure 3

Comparison of the measured and predicted annual groundwater drawdown in the test stages of the different used ANNs.

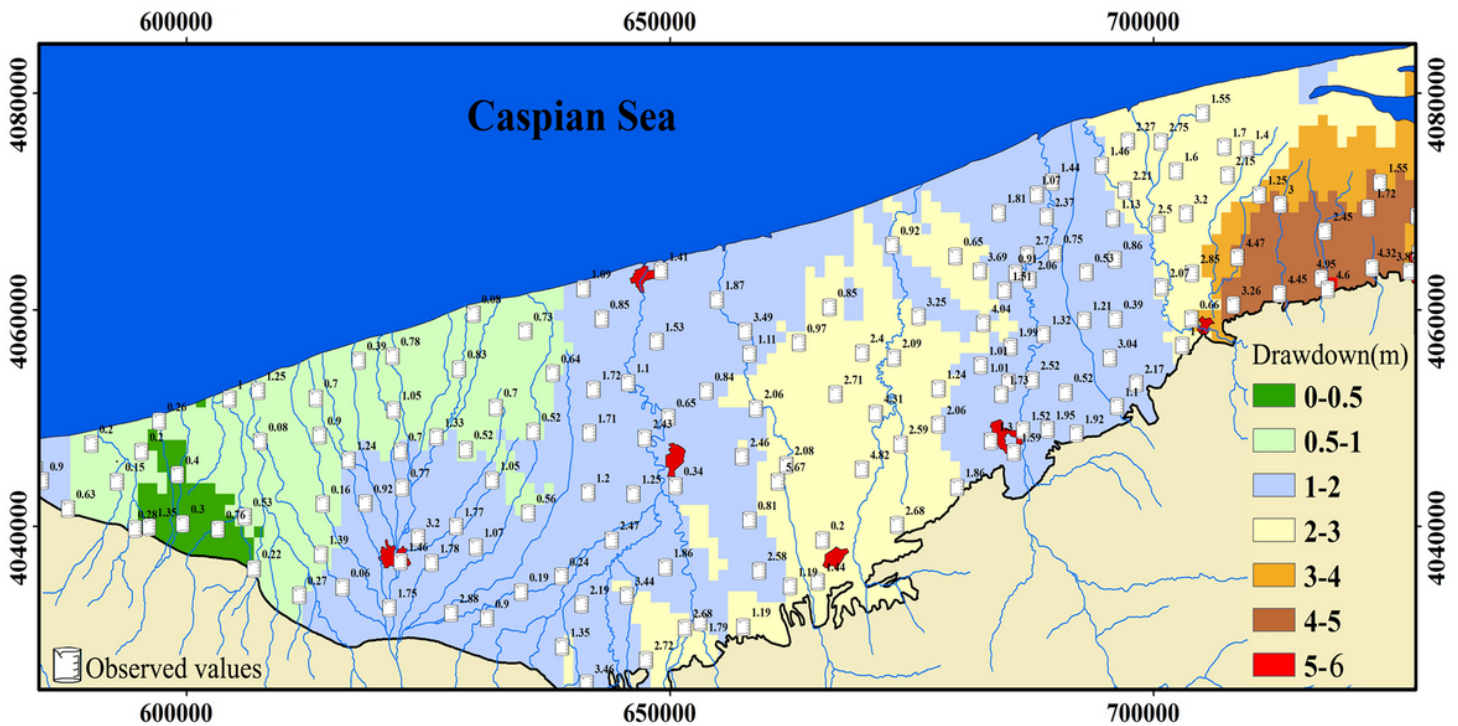


Figure 4

Map of the annual groundwater drawdown (m) in the study region. The observed values in the wells are also shown to assess the accuracy of the final map ($R\text{-sqr}=0.8$). Note: The designations employed and the presentation of the material on this map do not imply the expression of any opinion whatsoever on the part of Research Square concerning the legal status of any country, territory, city or area or of its authorities, or concerning the delimitation of its frontiers or boundaries. This map has been provided by the authors.